Optical-structural characteristics of i-ZnO thin films deposited by chemical route

F. K. Konan [1,2*], B. Hartiti [2], H. J. Tchognia Nkuissi [2,3], A. Boko[1]

[1]*Laboratoire d'Energie Solaire et de Nanotechnologie (LESN) - IREN (Institut de Recherches sur les Energies Nouvelles), Université Nangui Abrogoua, 02 BP 801 Abidjan, Côte d'Ivoire*
[2]*ERDyS Laboratory, GMEEMDD Group, FSTM, Hassan II Casablanca University, B.P 146, Mohammedia, Morocco*
[3] *Department of Physics, Faculty of Science, University of Yaoundé I, P.O Box 812, Yaoundé, Cameroon*

Abstract
i-ZnO thin films were deposited on glass substrates using sol-gel via dip-coating method. Characterization techniques such as X-ray diffraction (XRD), Scanning Electron Microscopy (SEM), Energy Dispersive X-ray spectroscopy (EDX) and UV/Vis/NIR spectrophotometer were used to investigate the optical-structural characteristics of the as-grown thin films. It was found grains with hexagonal shape and smooth surface grown over the substrate surface. The samples are composed of zinc (Zn) and oxygen (O) elements and the R-value estimated is 284.2%. The crystallographic orientation of i-ZnO thin films shows the preferred c-axis direction. Films were uniform and well adherent to the glass substrates. Grain size is found to be 35.34 nm with a low dislocation density about 0.8×10^{-3} nm^{-2}. Good optical quality of the films is manifested by transmittance spectra significantly larger than 90% in the visible wavelength region while the optical band gap energy is 3.322 eV. The experimental results confirm that chemical route dip-coating method succeeded in zinc oxide thin films deposition with high crystalline structure. These samples are suitable for potential applications in optoelectronic devices and transparent thin-film field-effect transistors.

1. Introduction

Oxide thin films of zinc oxide (ZnO), tin dioxide (SnO_2), cadmium sulphide (CdS), etc. have attracted great attention from both academic and industrial communities due to their enhanced characteristics for potential applications [1 - 6]. They have been used in many technical fields such as, varistors [2], piezoelectric transducers [3], gas sensors devices [4], transparent conducting windows in solar cell devices [5, 6], etc. One of these is zinc oxide (ZnO).

Zinc oxide is an II-VI group semiconductor family with c-axis oriented hexagonal wurtzite structure and is highly transparent and conductive as well as very chemically stable and biocompatible [7]. Additional characteristics include the abundance of source material which is inexpensive and non-toxic, high mechanical and thermal stabilities at room temperature, wide band gap (3.37 eV) associated to its large exciton binding energy (60 meV) [8]. Previous works reported that ZnO crystallites with preferential orientation are desirable for the above applications where crystallographic orientation (002) is a prerequisite condition for well oriented structure and exhibiting best properties [9 - 11]. A lot of methods have been extensively used for oriented ZnO films synthesis, including chemical bath deposition (CBD) [12], electrochemical process [13], thermal decomposition [14], molecular beam epitaxy (MBE) [15], micro-emulsion method [16], sol-gel techniques [17, 18], spray ultrasonic deposition [19], atomic layer deposition (ALD) [20], rf magnetron sputtering [21], etc. It is well known that ZnO thin films with high quality and uniformity were mostly realized with vapor phase growth techniques such as molecular beam epitaxy (MBE), pulsed laser deposition technique [15, 20, 21].

Nevertheless, these methods require expensive and sophisticated equipment set-up, and are characterized by high consumption of energy. Recently, opportunity is in sol-gel dip-coating synthesis which is a broadly used chemical synthesis route because of its easiness, repeatability, and low cost equipment [17, 18]. So far, dip-coating method is still an attractive deposition process of large area films on flat or cylindrical substrates.

Although there are several efforts around on dip-coating synthesis, it remains one of the utilized technique for synthesis and characterization of ZnO thin film [12 - 21]. The aim of this work was to deposit i-ZnO thin films using a simple dip-coating technique and characterize the as-grown films. The crystal structure, morphology and chemical composition of the products were characterized by means of X-ray diffraction (XRD), Scanning Electron Microscopy (SEM) with Energy Dispersive X-ray spectroscopy (EDX) and UV-Vis spectrophotometer scanner techniques.

2. Material and Methods

In a typical synthesis, ZnO thin films were prepared of 0.55 mol.L^{-1} zinc acetate dehydrate [$Zn(CH3COO)_2 \cdot 2H_2O$] and a mixture of ethanol and diethanolamine (DEA). The molar ratio of DEA to zinc acetate dehydrate was kept at 1.0. Before deposition, the glass substrates were ultrasonically cleaned with an acetone, isopropanol and finally with deionized water for 15 min in each step and then dried using compressed air.

The dip-coating process was achieved when cleaned glass substrates were gradually immersed into the solution, remaining inside about 20 s and then withdrawn at a rate of 6.0 cm/min at room temperature (300 K). After being deposited, the gel layers were heat-treated at 300°C for 10 min to evaporate the solvent and remove organic residuals. The procedures from coating to drying were repeated three times until the thickness of the sintered films was achieved. All the samples were subsequently annealed at 550 ^{o}C for 2 hours.

X-ray analysis of the coated thin films was carried out by XPERT-PRO X-ray diffractometer with copper target and Kα radiation (λ = 1.54060 Å) operating at 35.4 kV and 28 mA, where the diffracted X-ray intensities were recorded. The samples were scanned from 10 to 70° in steps of 0.0670°. Crystal structure, orientation and structural parameters, including crystallite size, dislocation density and lattice strain were estimated based on X-ray diffraction (XRD) line broadening of the most intense diffraction lines of the (002) plane. Scanning Electron Microscopy (SEM; JEOL, JSM-6700F used emitter voltage = 5 kV) was employed to reveal the microstructure and the surface morphology of ZnO thin film and Energy Dispersive X-ray spectroscopy (EDX) (EDX; Jeol JSM-6X60La, emitter voltage = 20 kV) was employed to study the chemical composition of the deposited ZnO thin films. Optical transmittance measurements were performed using UV-Vis spectrophotometer (Lambda-750, Perkin-Elmer, America) in the 300-800 nm wavelength range.

3. Results and discussion

3.1. Elemental analysis

EDX measurements were performed to study the elemental composition of the as-grown thin films. The EDX spectrum result as presented in Figure 1 provides two peaks corresponding to zinc (Zn) and oxygen (O) elements. Some impurities (Si, Ca) are found in the spectrum which are originated from the glass substrate [22]. The inset of Figure 1 presents the weight and atomic percent compositions (Wt% and At%) of the constituents of zinc oxide nanoparticles i.e. Zn and O atoms. The R-value (i.e., At% ratio of O^{2-} to Zn^{2+}), calculated for prepared ZnO nanoparticles is 284.2%. In fact, ZnO is considered as an n-type semiconductor where most defects are zinc interstitials (Zn_i) and oxygen vacancy (V_O). Excess of oxygen and deficiency of zinc in the films prepared were observed in this work, which could possibly be attributed to the O_i in ZnO thin films. These samples may give rise to less observed p-type semiconducting behaviour.

3.2. X-ray diffraction

X-ray diffraction pattern of i-ZnO is presented in Figure 2. As it can be seen, the XRD pattern of the film shows the single (002) peak at diffraction angle 2θ equal to 34.46°. From the pattern, it could be

concluded that ZnO films were completely crystallized to hexagonal wurtzite structure with preferred (002) orientation (compared with Joint Committee on Powder Diffraction Standards, Card No. 36-1451) [23]. No other peak was detected in the pattern, indicating that high-purity i-ZnO films were fabricated [22]. The full-width at half-maximum (FWHM) value of the (002) diffraction peak was found to be 0.2412°, demonstrating that the crystalline quality of the film gets better and good adhesion to glass substrate was achieved [18]. In addition, previous reported works [24, 25] showed that the degree of c-axis orientation of the ZnO thin films was strongly dependent on the initial zinc concentration and films were preferentially oriented in the c-axis, or (002) plane, for zinc oxide concentrations in the range of 0.3-0.6 mol.L^{-1}.

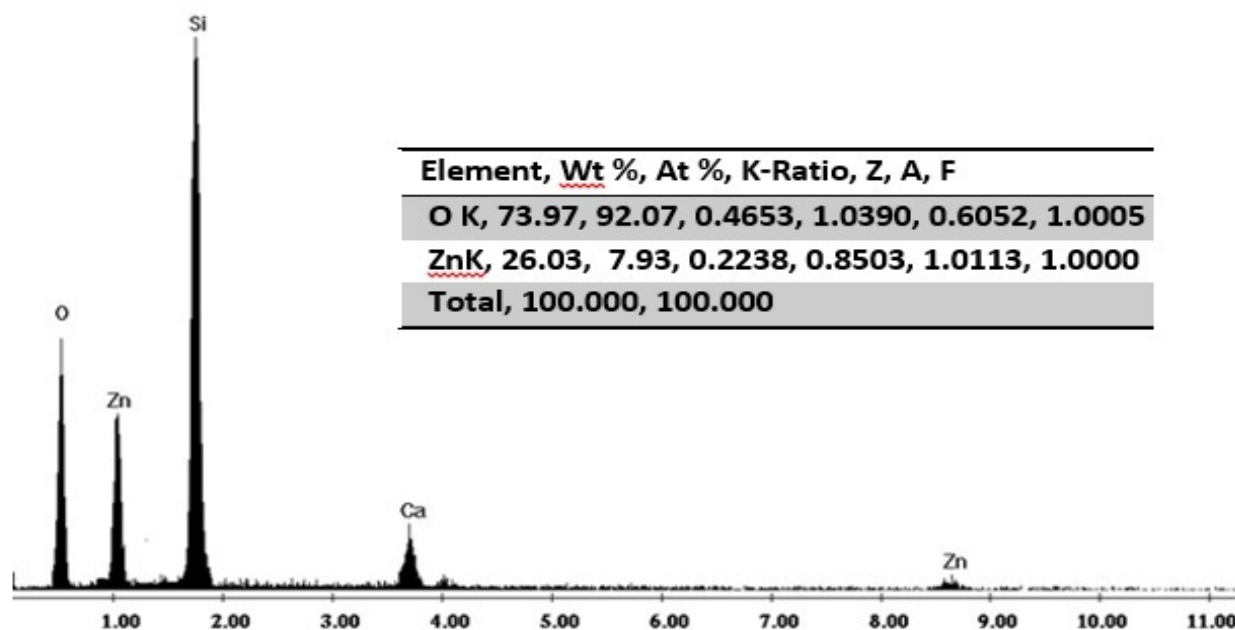| Element, Wt %, At %, K-Ratio, Z, A, F |
| O K, 73.97, 92.07, 0.4653, 1.0390, 0.6052, 1.0005 |
| ZnK, 26.03, 7.93, 0.2238, 0.8503, 1.0113, 1.0000 |
| Total, 100.000, 100.000 |

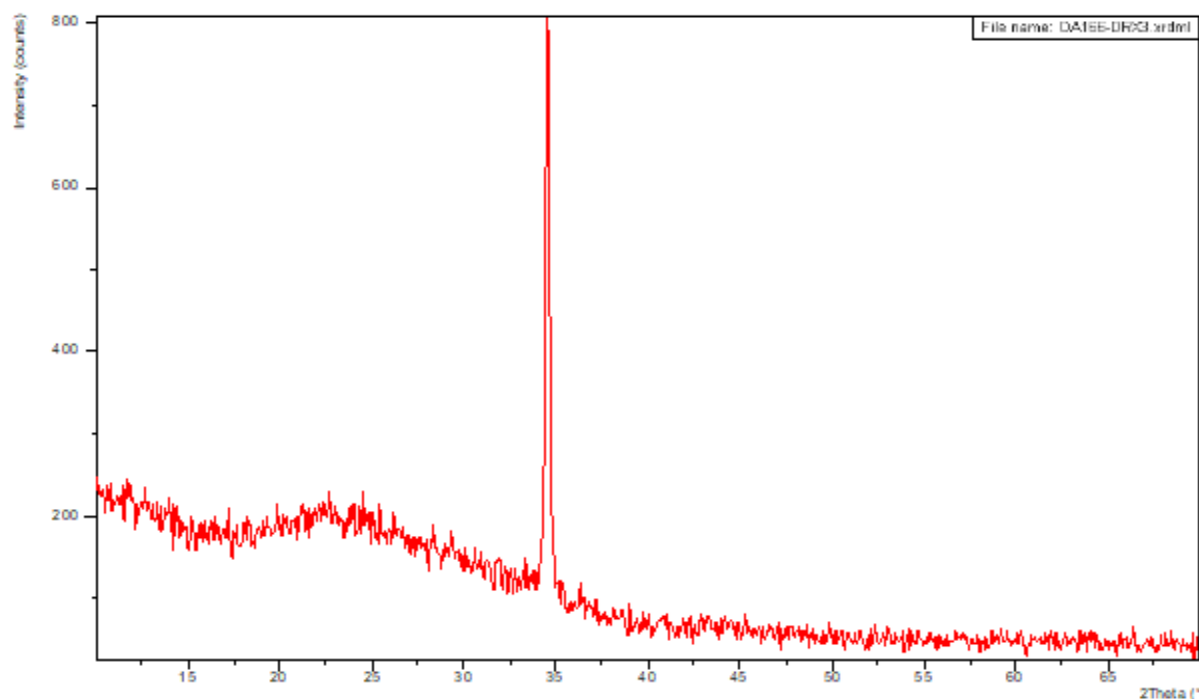**Figure 1:** EDX spectrum of coated zinc oxide thin film

Figure 2: XRD pattern of zinc oxide thin film

The mean average crystallite size (D) along the preferentially oriented crystal plane (002) was calculated using the well-known Scherrer formula [26]:

$$D = \frac{0.9\lambda}{\beta\cos\theta} \qquad (1)$$

Where λ is the X-ray wavelength (1.54060Å), θ is the Bragg diffraction angle in degrees and β is the full width at half maximum (FWHM) of (hkl) crystallographic orientation.

The value of crystallite size as tabulated in Table 1, is in good agreement with previous report [19].

The shift in diffraction angle 2θ to higher value is due to internal stress, film defects and lower densification. In materials science, the dislocation density is a measure of crystallographic defect or irregularity, within a crystal structure, and also defined as a topological defect [27]. The dislocation density (δ) value was evaluated using the following relation [28]:

$$\delta = \frac{1}{D^2} \qquad (2)$$

The FWHM of the XRD peaks may also contain contributions from lattice strain. The lattice average strain of the films was calculated using the Stokes-Wilson relation [29]:

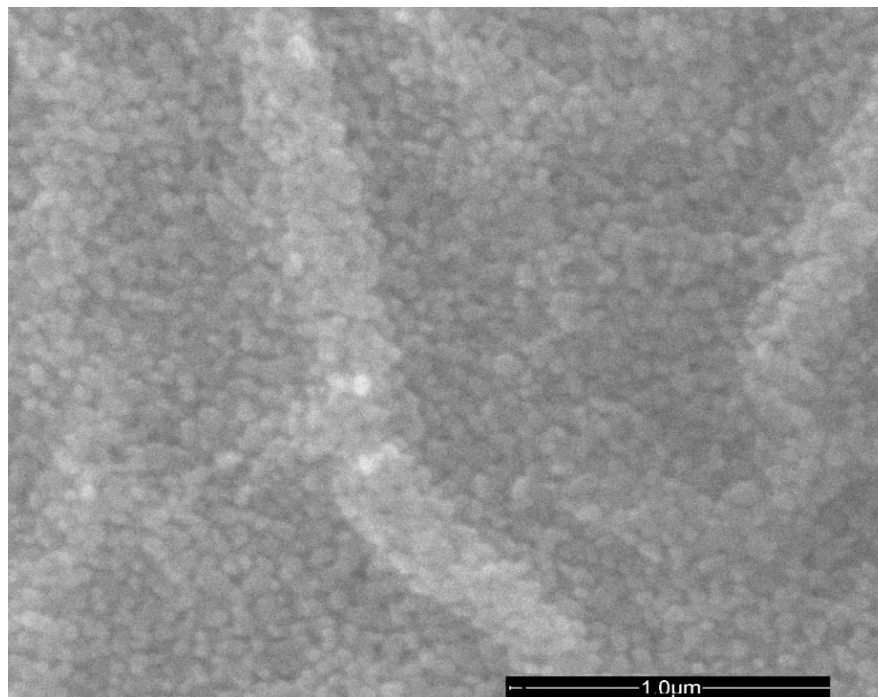$$\varepsilon = \frac{\beta_{hkl}}{4\tan\theta_{hkl}} \qquad (3)$$

The Data obtained from XRD of the as-grown samples are summarized in Table 1.

Table 1: Data obtained from XRD

2θ (°)	(hkl)	FWHM β (002) (°)	crystallite size (D) (nm)	Dislocation density δ (x 10⁻³) (nm⁻²)	Strain ε (%)
34.46	(002)	0.2412	35.34	0.8	- 0.3192

3.3. Surface morphology

The surface morphology of the films was examined using Scanning Electron Microscopy (SEM). Figure 3 presents the SEM image representative of the ZnO thin film as grown.
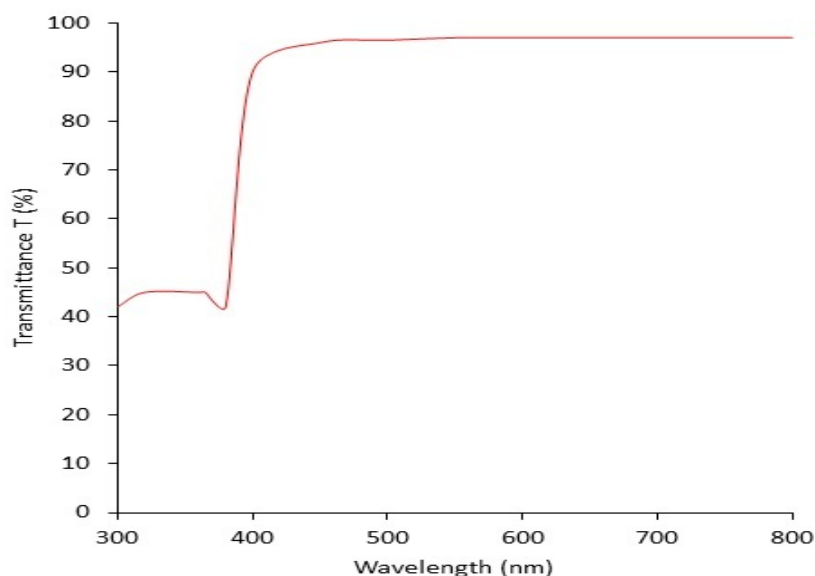

Figure 3: SEM image of coated zinc oxide thin film

Homogeneous nano-spherical grains are formed with surfaces covered with non-uniformly distributed grains. We can observe dark as well as lighted areas.

The grains observed by SEM are formed by the aggregation of micro-crystallites whose preferential tendency orientation is the c-axis perpendicular to glass substrate surface [23]. The image of the ZnO film as it is grown reveals that the film consists of a morphology formed of grains with an almost smooth surface.

3.4. Optical properties

Figure 4 shows the transmittance of the ZnO thin films. All the films exhibited a high transmittance in the visible spectral range. The absorption edges in the UV-Vis region of the samples can be observed clearly, including absorption region of ZnO (385 nm~400 nm). The average optical transmittance in the visible region was found to be in the order of approximately 95 % suggesting the absence of scattering or absorption of the incident light.
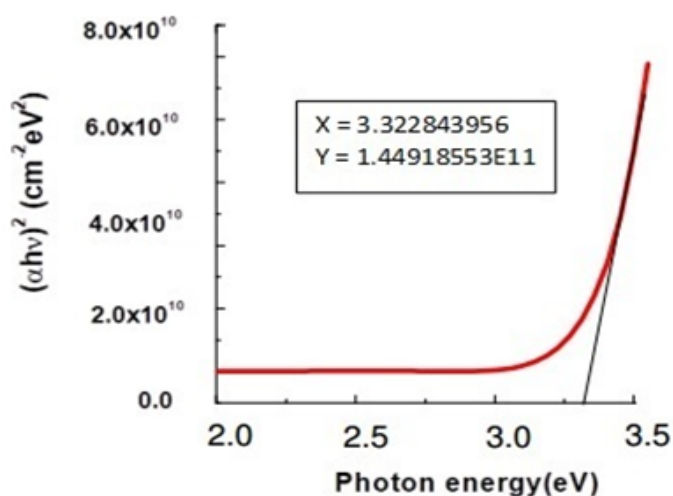

Figure 4: Optical transmittance spectra of i-ZnO thin film

According to results reported, zinc oxide exhibits direct band and the absorption coefficient (α) follows Tauc relation [31]:

$$(\alpha h\upsilon)^2 = A(h\upsilon - E_g) \qquad (4)$$

Where E_g is the optical band gap, h is Planck's constant, υ is the frequency of the incident photon and A is a constant which depends on the electron-hole mobility.

X = 3.322843956
Y = 1.44918553E11

Figure 4: Optical band gap value determination of i-ZnO thin film

The optical band gap is determined by extrapolation of the linear region from the α^2 versus $h\upsilon$ plot near the onset of the absorption edge to the energy axis. The resulting value for the as-grown i-ZnO thin film is 3.322 eV. It is clear that the optical band gap measured is inferior to 3.37 eV, but it correlates well with the known literature data [32, 33]. In general, the optical band gap shifted due to the carrier concentrations in the films because defined by Burstein-Moss effect [34].

Conclusion

We have succeeded to grow i-ZnO thin films on glass substrate using a simple sol-gel via dip-coating technique. The as-deposited films exhibited a hexagonal wurtzite structure with (002) preferential orientation. The grain size is found to be 35.34 nm. A low dislocation density about 0.8×10^{-3} nm^{-2} was detected. SEM micrograph of i-ZnO thin film shows grains with hexagonal shape and smooth surface. The constituents of the films are zinc (Zn) and oxygen (O) atoms, and the R-value estimated is 284.2%. In addition, the average transmittance of the samples is larger than 90% in the visible wavelength range while the optical band gap energy is 3.322 eV.

The i-ZnO thin films prepared in this work have good optical-structural characteristics for potential applications in optoelectronic devices and transparent thin-film field-effect transistors.

References

1. C-Y. Tsay, S-T. Chen, M-T. Fan, Solution-Processed Mg-Substituted ZnO Thin Films for Metal-Semiconductor-Metal Visible-Blind Photodetectors. *Coatings* 9(2019)277-291. doi:10.3390/coatings9040277

2. V. Balaprakash, P. Gowrisankar, S. Sudha & R. Rajkumar, Aluminum doped ZnO transparent conducting thin films prepared by sol-gel dip coating technique for solar cells and optoelectronic applications, *Mater. Technol.* 33 (2018) 410-420 https://doi.org/10.1080/10667857.2018.1455384

3. P. Nagaraju, Y. Vijayakumar, M.V. Ramana Reddy, U.P. Deshpande, Effect of vanadium pentoxide concentration in ZnO/V_2O_5 nanostructured composite thin films for toluene detection, *RSC Adv.* 9 (2019) 16515-16524. DOI: 10.1039/C9RA02356A

4. C. de Julian Fernandez, M. G. Manera, G. Pellegrini, M. Bersani, G. Mattei, R. Rella, L. Vasanelli, P. Mazzoldi, Surface plasmon resonance optical gas sensing of nanostructured ZnO films, *Sensor. Actuat. B: Chem* 130 (2008) 531-537. https://doi.org/10.1016/j.snb.2007.09.065

5. K. Matsubara, P. Fons, K. Iwata, A. Yamada, K. Sakurai, H. Tampo, S. Niki, ZnO transparent conducting films deposited by pulsed laser deposition for solar cell applications, *Thin Solid Films* 431-432 (2003) 369-372. https://doi.org/10.1016/S0040-6090(03)00243-8

6. S. Alhammadi, H. Park, W. K. Kim, Optimization of Intrinsic ZnO Thickness in Cu(In,Ga)Se2-Based Thin Film Solar Cells, *Materials* 12 (2019) 1365-1381. https://doi.org/10.3390/ma12091365

7. K. Sivalingam, P. Shankar, G.K. Mani, J.B.B. Rayappan, *Mater. Lett.* 134 (2014) 47-50. https://doi.org/10.1016/j.matlet.2014.07.019

8. C. Klingshirn, ZnO: From basics towards applications, *Phys. Status Solidi B* 244(9) (2007) 3027-3073. https://doi.org/10.1002/pssb.200743072

9. L. Zhang, Y. Ruan, Y. Liu, Y. Zha, Effect of growth temperature on the structure and optical properties of ZnO nanorod arrays grown on ITO substrate, *Cryst. Res. Technol.* 48(11) (2013) 996-1002. https://doi.org/10.1002/crat.201300216

10. R. Romero, D. Leinena, E.A. Dalchiele, J.R. Ramos-Barrado, F. Martín, The effects of zinc acetate and zinc chloride precursors on the preferred crystalline orientation of ZnO and Al-doped ZnO thin films obtained by spray pyrolysis, *Thin Solid Films* 515 (2006) 1942-1949. https://doi.org/10.1016/j.tsf.2006.07.152

11. P.-M. Martin, M.S. Good, J.W. Johnston, G.J. Posakony, L.J. Bond, S.L. Crawford, Piezoelectric films for 100-MHz ultrasonic transducers, *Thin Solid Films* 379 (2000) 253-258. doi.org/10.1016/S0040-6090(00)01339-0

12. N. Winkler, S. Edinger, W. Kautek, T. Dimopoulos, Mg-doped ZnO films prepared by chemical bath deposition, *J. Mater. Sci.* 53(7) (2018) 5159- 5171. https://doi.org/10.1007/s10853-017-1959-8

13. A. Rezaee, R. Darvishi Cheshmeh Soltani, A.R. Khataee, H. Godini, Optimization of combined photocatalytic involving immobilized ZnO nanoparticles and electrochemical processes for ammoniacal nitrogen removal from aqueous solutions, *J. Mater. Environ. Sci.* 3(5) (2012) 955-966

14. Y. Yang, X. Li, J. Chen, H. Chen, X. Bao, ZnO nanoparticles prepared by thermal decomposition of β-cyclodextrin coated zinc acetate, *Chem. Phys. Lett.* 373 (2003) 22-27. doi.org/10.1016/S0009-2614(03)00562-1

15. F.X. Xiu, Z. Yang, L.J. Mandalapu, J.L. Liu, p-type ZnO films with solid-source phosphorus doping by molecular-beam epitaxy, *Appl. Phys. Lett.* 88 (2006) 052106-3. doi.org/10.1063/1.2170406

16. Ö.A. Yıldırım, C. Durucan, Synthesis of zinc oxide nanoparticles elaborated by microemulsion method. *J. Alloys Comp.* 506(2) (2010) 944-949. doi:10.1016/j.jallcom.2010.07.125

17. R.A. Bari, P.A. Bari, R.H. Bari, Studies on Sol-gel Dip-coated Nanostructured ZnO Thin Films, *J. Nanostruct.* 9(2) (2019) 326-330. DOI: 10.22052/JNS.2019.02.014

18. F.K. Konan, J.S. N'cho, H.J. Tchognia Nkuissi, B. Hartiti, A.Boko, Influence of the precursor concentration on the morphological and structural properties of zinc oxide (ZnO), *Mater. Chem. Phys.* 229 (2019) 330-334. https://doi.org/10.1016/j.matchemphys.2018.12.082

19. S. Benramache, Y. Aoun, A. Charef, B. Benhaoua, S. Lakel, Transition width effect on optical characterizations of ZnO thin films deposited by spray ultrasonic, Inorganic and Nano-Metal Chem. 49(6) (2019) 177-181. https://doi.org/10.1080/24701556.2019.1624568

20. P. Listewnik, M. Hirsch, P. Struk, M. Weber, M. Bechelany, M. Jedrzejewska-Szczerska, Preparation and Characterization of Microsphere ZnO ALD Coating Dedicated for the Fiber-Optic Refractive Index Sensor, *Nanomaterials* 9 (2019) 306-317. https://doi.org/10.3390/nano9020306

21. J-W. Hoon, K.-Y. Chan, J. Krishnasamy, T.-Y. Tou, D. Knipp, Direct current magnetron sputter-deposited ZnO thin films, *Appl. Surf. Sci.* 257(7) (2011) 2508-2515. doi:10.1016/j.apsusc.2010.10.012

22. A.A. Ahmad, A.M. Alsaad, Q.M. Al-Bataineh, M.A. Al-Naafa, Optical and structural investigations of dip-synthesized boron-doped ZnO-seeded platforms for ZnO nanostructures, *Appl. Phys. A* 124 (2018) 458-471. https://doi.org/10.1007/s00339-018-1875-z

23. B. Post, S. Weissmann and H F McMurdie H F (eds.), Joint Committee on Powder Diffraction standards, Inorganic Vol., Card No. 36-1451, International Centre for Diffraction Data, Swarthmore, PA, 1990.

24. X. Lu, K. Kanamori, K. Nakanishi, Preparation of zinc oxide with three-dimensionally interconnected macroporous structure through sol-gel method accompanied by phase separation, *New J. Chem.* 43 (2019) 11720-11726. doi:10.1039/c9nj02373a

25. S. Kaur, M. Deshwa, Study of Molarity Concentration Variation Over Optical, Structural and Gas Sensing Response for ZnO Thin Film Based NOx Gas Sensor, *Transactions on Electrical and Electronic Materials* 20 (2019) 309-314. https://doi.org/10.1007/s42341-019-00113-x

26. P. Bindu, S. Thomas, Estimation of lattice strain in ZnO nanoparticles: X-ray peak profile analysis, *J. Theor. Appl. Phys.* 8 (2014) 123-134. DOI 10.1007/s40094-014-0141-9

27. D. Thapa, D.J. Huso, J.L. Morrison, C.D. Corolewski, M.D. McCluskey, L. Bergman, Achieving highly-enhanced UV photoluminescence and its origin in ZnO nanocrystalline films, *Opt. Mater.* 58 (2016) 382-389. https://doi.org/10.1016/j.optmat.2016.05.008

28. M. Shaban, M. Zayed, H. Hamdy, Nanostructured ZnO thin films for self-cleaning applications, *RSC Adv.* 7(2) (2017) 617-631. DOI: 10.1039/C6RA24788A

29. S.N. Danilchenko, O.G. Kukharenko, C. Moseke, I.Y. Protsenko, L.F. Sukhodub, B. Sulkio-Cleff, Determination of the Bone Mineral Crystallite Size and Lattice Strain from Diffraction Line Broadening, *Cryst. Res. Technol.* 37(11) (2002) 1234-1240. doi:10.1002/1521-4079(200211)37:11<1234::aid-crat1234>3.0.co;2-x

30. B.J. Babu, A. Maldonado, S. Velumani, R. Asomoza, Electrical and optical properties of ultrasonically sprayed Al-doped zinc oxide thin films, *Mater. Sci. Eng. B* 174 (2010) 31-37. doi.org/10.1016/j.mseb.2010.03.010

31. I. Musa, N. Qamhieh, Study of optical energy gap and quantum confinement effects in zinc oxide nanoparticles and nanorods, *Digest Journal of Nanomaterials and Biostructures* 14 (2019) 119-125.

32. A. Riaz, A. Ashraf, H. Taimoor, S. Javed, M.A. Akram, M. Islam, M. Mujahid, I. Ahmad, K Saeed, Photocatalytic and Photostability Behavior of Agand/or Al-Doped ZnO Films in Methylene Blue and Rhodamine B under UV-C Irradiation, *Coatings* 9 (2019) 202-217. doi:10.3390/coatings9030202

33. A.P. Rambu, D. Sirbu, A.V. Sandu, G. Prodan, V. Nica, Influence of In doping on electro-optical properties of ZnO films, *Bull. Mater. Sci.* 36(2) (2013) 231-237. https://doi.org/10.1007/s12034-013-0471-2

34. P.K. Chakraborty, G.C. Datta, K.P. Ghatak, The simple analysis of the Burstein–Moss shift in degenerate n-type semiconductors, *Physica B: Condensed Matter* 339 (2003) 198-203. doi.org/10.1016/j.physb.2003.07.001

(2019) ; http://www.jmaterenvironsci.com